Analyzing Spatio-temporal Land Cover Dynamics in an Atlantic Forest Portion Using Unsupervised Change Detection Techniques

Gabriela Ribeiro Sapucci[1] · Rogério Galante Negri[1] · Wallace Casaca[1] · Klécia Gili Massi[2]

Abstract

Over the past decades, the Southeast Atlantic Forest in Paraíba do Sul River Valley has suffered intense deforestation and human disturbances. Due to the Atlantic Forest biodiversity and the economic relevance of such a region in Brazil, spatial-temporal analyses are of crucial importance to protect the forest, as well as to support economic decision-making of public and private agents. In this context, the use of change detection techniques applied to remote sensing imagery arises as a powerful tool to track and map the Earth's surface transformations. Therefore, this work investigates the effectiveness and practical feasibility of distinct unsupervised change detection approaches when they are applied to reveal the spatial-temporal dynamics in Paraíba do Sul River Valley across the last four decades. Different change detection approaches such as Change Vector Analysis (CVA), a K-Means and Principal Component Analysis (PCA-KM) framework, and a Alternating Sequential Filtering (ASF) based process were taken and properly tuned to cope with Landsat image series. The analysis of the results revealed a permanent land cover change rate over the last decades. Moreover, these changes do not necessary occur in the same locations, as it was confirmed the existence of successive modifications in original coverage of the study area. Another observed aspect is that the simplest technique for detecting changes, CVA, turned out to be the best approach to map the changes in the examined region.

Keywords Change detection · Unsupervised · Multitemporal analysis · Landsat imagery · Remote sensing

1 Introduction

The Paraíba do Sul River Valley is a very affluent and prosperous region in Brazil, located between São Paulo and Rio de Janeiro states [1]. The region is the home of a huge piece of the Atlantic Forest, one of the major biodiversity hotspots in the world with many endemic and endangered species [2]. Despite its high biodiversity and ecological importance, the Atlantic Forest has experienced alarming levels of habitat destruction and fragmentation, mainly due to the disorderly growth of agricultural and industrial activities [3–5]. According to SOS Mata Atlântica Foundation [6] – a Brazilian NGO dedicated to conserving this biome, the deforestation of Atlantic Forest is critical, as only 12.4% of the biome's native vegetation still remains undisturbed. This devastation scenario has contributed to transform the forest landscape into anthropic spaces, as well as to promote the fragmentation of its green zones [7]. As a result, the biome formations are not very representative in the so-called Paraíba Valley, since they have been substantivally altered over the time so that only a reduced number of green areas remains totally preserved.

The region has undergone different changes over the past few centuries, from the coffee growing in 19th-20th centuries to the eucalyptus cultivation nowadays. Coffee crop had its "gold century" between 1830-1930, promoting prosperity to the Paraíba Valley economy, but with the high price of Atlantic Forest deforestation. Due to the urban and industrial expansion, coffee culture was weakened, leading to the predominance of extensive pastures in the region. Moreover, the coffee productivity reduction triggered an intense rural exodus to large urban centers around the Paraíba Valley so that many of the abandoned lands were converted into small vegetation areas, thus partially contributing to the increase of forest coverage [8]. From 1966 to 1974, there was an exponential

✉ Rogério Galante Negri
  rogerio.negri@unesp.br

1   Institute of Science and Technology, São Paulo State University (Unesp), São José dos Campos, São Paulo, Brazil

2   Department of Energy Engineering, São Paulo State University (Unesp), Rosana, São Paulo, Brazil

growth in eucalyptus culture, encouraged by tax incentives given by the Brazilian government for reforestation projects, in particular, eucalyptus crops. Nowadays, the Paraíba Valley has a dense concentration of eucalyptus plantations which is an important economic pilar for the region [7].

Among several technologies that may support Spatio-temporal analysis of Paraíba Valley, the use of change detection techniques arises as a convenient alternative. Such techniques allow the identification of differences in multitemporal imagery acquired by Remote Sensing. Moreover, if the identification process is unsupervised, no ground-truth data is required so that the output will be a mapping which highlights the regions of the image where changes have occurred. Unsupervised change detection techniques have been successfully applied for different purposes, such as crop mapping [9, 10], forestry monitoring [11, 12], natural disasters inspection [13, 14], and urban planning [15, 16].

Considering the highly changeable scenario as faced by Paraíba Valley during the last decades, a descriptive study focused on identifying spatial-temporal changes in land use/cover of Atlantic Forest is proposed in this paper. We take a remote sensing imagery to perform multi-temporal analysis of the region, allowing for capturing different representations of large aerial areas in the Atlantic Forest as the time varies.

More specifically, we tune and run three unsupervised change detection approaches so as to collect several data-driven evidences to support specialists and public agents in the task of monitoring the Atlantic Forest ecozone. Also, we provide pair-wise and multiple instant comparisons in order to properly determine the dynamics of land changes. In our study, we adopt aerial images collected from the Landsat-5 and -8 satellites by the Thematic Mapper (TM) and Operational Land Imager (OLI) sensors. In particular, we compare the years 1987, 1997, 2007 and 2017.

This paper is organized as follows: Sect. 2 brings an introductory review about the change detection methods we apply to generate the results, while Sect. 3 describes the study area, data sets, and methodological aspects of the study. Section 4 presents the results and their discussion. Finally, Sect. 5 summarizes our findings and conclusions.

2 Unsupervised Change Detection Techniques

Change detection accomplishes the identification of changes in land surfaces through images acquired during a given time period [17]. This task plays a fundamental role in environmental studies, for example, to track the ecosystem transitions, as well as to better comprehend the successive interaction between natural phenomena and human activities. Once these changes are identified and properly quantified, the land use and land cover analysis can be performed in a more effective and comprehensive way [18].

Several change detection techniques have been proposed in the literature. We can roughly group these techniques between supervised and unsupervised ones. Due to specific constraints and limitations, which include high financial costs and the annalistic efforts to get a large amount of data to validate a supervised method, recently the scientific community has focused on unsupervised learning-based strategies [19]. Indeed, the ability of identifying temporal changes without any additional data resource makes unsupervised methods more attractive than the supervised-based ones [20, 21]. On the other hand, the unsupervised change detection methods are not able to discriminate land cover types behind the change or non-change events.

Usually, these techniques embrace post-classification analysis, simple arithmetic operations, Principal Component Analysis (PCA) and morphological filters [22]. In the following, we discuss each one of these change detection strategies.

2.1 Change Vector Analysis

The so-called Change Vector Analysis (CVA) [23] is an unsupervised learning-based model which comprises three successive steps. First, geometric and radiometric corrections are performed on an input pair of images. Thereby, let us denote by $\mathcal{I}^{(1)}$ and $\mathcal{I}^{(2)}$ the pair of the calibrated images, defined on a support $\mathcal{S} \subset \mathcal{N}^2$ of a given geographic region whose the position $s \in \mathcal{S}$ (i.e., a pixel) in $\mathcal{I}^{(1)}$ and $\mathcal{I}^{(2)}$ defines attribute vectors $\mathbf{x}_s^{(1)}$ and $\mathbf{x}_s^{(2)}$, respectively. These vectors embed a particular measures computed from a specific target regarding different wavelength intervals.

Next, $\mathcal{I}^{(1)}$ and $\mathcal{I}^{(2)}$ are compared through the vectors $\mathbf{x}_s^{(1)}$ and $\mathbf{x}_s^{(2)}$ for all $s \in \mathcal{S}$. The amplitude difference $\|\mathbf{x}_s^{(1)} - \mathbf{x}_s^{(2)}\|$ gauges how similar $\mathbf{x}_s^{(1)}$ and $\mathbf{x}_s^{(2)}$ are, producing the resulting difference image $\mathcal{I}^{(1-2)}$. Finally, the discrimination between the relevant and irrelevant features of the images is performed, by exploiting the difference image $\mathcal{I}^{(1-2)}$. Relevant differences, usually with high magnitudes, stands for changes, while low magnitude differences correspond to non-change events. We denote changes and non-changes by the classes ω_c and ω_n, respectively. The use of thresholding techniques, for example, the Otsu [24] or Kittler-Illinghworth [25] algorithms, allows learning-based strategies to distinguish between the low and high magnitude differences.

2.2 PCA and K-Means framework

The well-known mathematical model Principal Component Analysis (PCA) [26] has been the basis of many unsupervised change detection methods [27–29]. A good representative

of PCA-based method is the one proposed in [30], which combines the versatility of PCA with the effectiveness of K-Means (KM) clustering [31] into a unique unsupervised change detection approach. Despite its simplicity in terms of algorithmic architecture, the method does a very good job in identifying changes while still keeping robust to noisy data.

Similar to CVA, typical PCA-based approaches rely on an amplitude difference image $\mathcal{I}^{(1-2)}$ built from a pair of images $\mathcal{I}^{(1)}$ and $\mathcal{I}^{(2)}$ with support $\mathcal{S}$. First, the domain $\mathcal{S}$ is decomposed into non-overlapping squares of dimensions $h \times h$, where $h = 2k + 1; k \geq 2$. Next, a vectorial representation for each image region in $\mathcal{I}^{(1)}$ and $\mathcal{I}^{(2)}$ is derived so that the PCA is computed on this set of vectors. This is also performed for each pixel s in the composite difference image $\mathcal{S}$ of $\mathcal{I}^{(1-2)}$. The extracted vectors are then projected onto a different feature space by the PCA technique, wherein the first p components are taken. Finally, the KM algorithm is applied on the projected data so that two clusters are derived. The cluster of the centroid closer to the origin of the projection space determines the set of non-change pixels (ω_n), while the remaining cluster stands for the pixels that have been changed (ω_c).

Here, we refer to the combination of PCA and K-Means as PCA-KM.

2.3 Alternating Sequential Filters for Change Detection

The use of morphological filters, especially the class of Alternating Sequential Filters (ASF), arises as a valid alternative to perform change detection tasks. ASF consists in a sequence of opening and closing morphologic operations so that the images are filtered several times in order to capture their objects of interests [32, 33]. By applying ASF, one can highlight the differences between images while preserving the geometric features of the targets in the image [19].

For instance, in Mura et al. [19], the authors proposed an unsupervised change detection method inspired on the ASF concepts. Analogously to CVA and PCA-KM, their method computes the amplitude difference image $\mathcal{I}^{(1-2)}$, and then the ASF is applied to reduce the high-intensity values of $\mathcal{I}^{(1-2)}$, as well as to preserve the geometric features of the difference image. The ASF filtering operations are successively applied based on gradual increases of the kernel size. Notice that ASF takes the number of iterations as a free parameter, which is used to regulate the change detection capability of the method.

Lastly, the Kittler-Illinghworth thresholding then applied to the ASF filtering result from $\mathcal{I}^{(1-2)}$. While filtered pixel values inferior to the defined threshold are classified as non-changes (ω_n), pixels whose values are greater than such threshold are assigned to change locations (ω_c).

For the sake of simplicity, we denote this method as ASF.

3 Data and Experiment Design

In this section, we detail the data sets and the methodological steps we have conducted in this study. Specifically, Subsection 3.1 describes the study area and the examined data, while Subsection 3.2 presents the experiment design.

3.1 Study Area Description

The study area covers the Metropolitan Region of Paraíba do Sul River Valley, in Brazil, a region located between São Paulo and Rio de Janeiro cities which encompasses an area of 14,236 km^2, with a population of approximately two million people [34]. Figure 1 depicts the study area

Fig. 1 The study area location
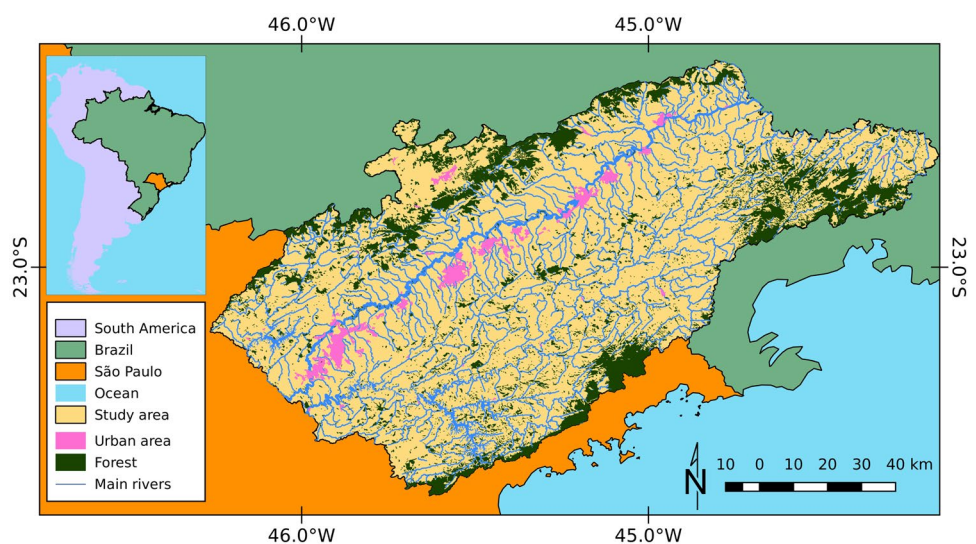
location. According to Silva et al. [8], the study area has been undergoing a forest transition process, migrating from a period of constant reduction of native vegetation to the natural expansion of genuine forest territories, which is related to the abandonment of deep slope areas that are not compatible with mechanized agriculture, demographic and economic aspects.

As previously discussed in Sect. 1, Paraíba do Sul River Valley is the home of the Atlantic Forest, but nowadays such a green coverage of this biome is highly fragmented [6]. The current scenario is the result of intense deforestation caused by anthropic activities over the years [4].

We take images acquired by the TM and OLI sensors aboard the Landsat-5 and -8 satellites, respectively. These images refers to the study area in the years of 1987, 1997, 2007 and 2017. The aerial scenes from 1987 to 2007 were acquired by the TM sensor (Landsat-5), while the 2017 image was acquired by the OLI sensor (Landsat-8). The images have a spatial resolution of 30m and spectral bands from blue and short-wave infrared wavelengths. Additionally, the full data was obtained from the EarthExplorer platform [35] and express the surface reflectance after the atmospheric correction has been performed by LEDAPS [36] and LaSRC [37] algorithms. Finally, the output data produced by such algorithms were used to properly detect clouds and shadows masks in the images for each time instant.

Because of the large-size dimensions of the study area, we generate composite image mosaics to carefully inspect all the region. Four scenes were taken to produce each mosaic. These scenes were chosen in the months of August and September in order to ensure low occurrence of clouds and similar solar incidence. Figure 2 illustrates the resulting

Table 1 Summary of change and non-change samples in different periods

| Class	Period (# of pixels/# of polygons)			
	1987–1997	1997–2007	2007–2017	1987–2017
Change (ω_c)	556/20	505/14	323/12	113/6
Non-change (ω_n)	1444/23	952/22	972/14	525/12

mosaics for the analyzed years. Each mosaic is defined on a wide support of 7800×4650 pixels. The studied region has around 17.27 millions of pixels.

Assuming the interest in conducting quantitative assessments of the change detection results, it makes necessary the availability of ground-truth samples. Under this premise, a detailed inspection and comparison of the study area mosaics in different pairs of years were carried out, by selecting samples over locations where occur and do not occur changes. Also, the land use and land cover maps provide by MapBiomas project [38] supported the process of comparing pairs of instants and identifying candidate regions for samples collection. Table 1 summarizes the selected samples in the four pairs of periods. Notice that, once the sample dimensions are much smaller than the entire region, we can not illustrate in details the spatial distribution of these samples.

3.2 Experiment Design

Figure 3 illustrates the experiment design of this study. From the mosaics in Fig. 2, and by applying the change detection methods already discussed in Sections 2.1-2.3, we generated temporal changes/non-changes maps for different pairs of instants. In

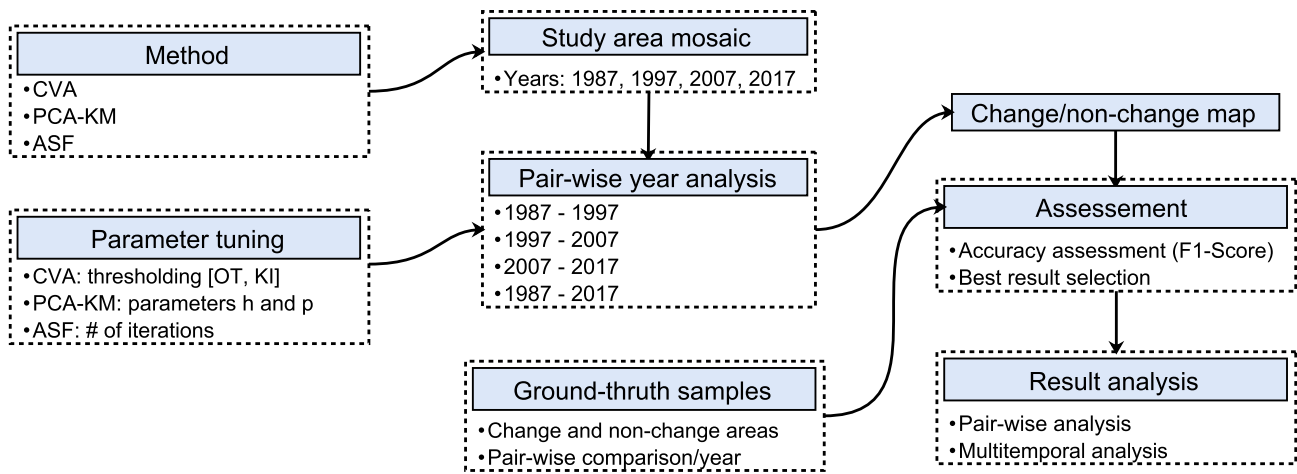**Fig. 2** The study area time-serie mosaics
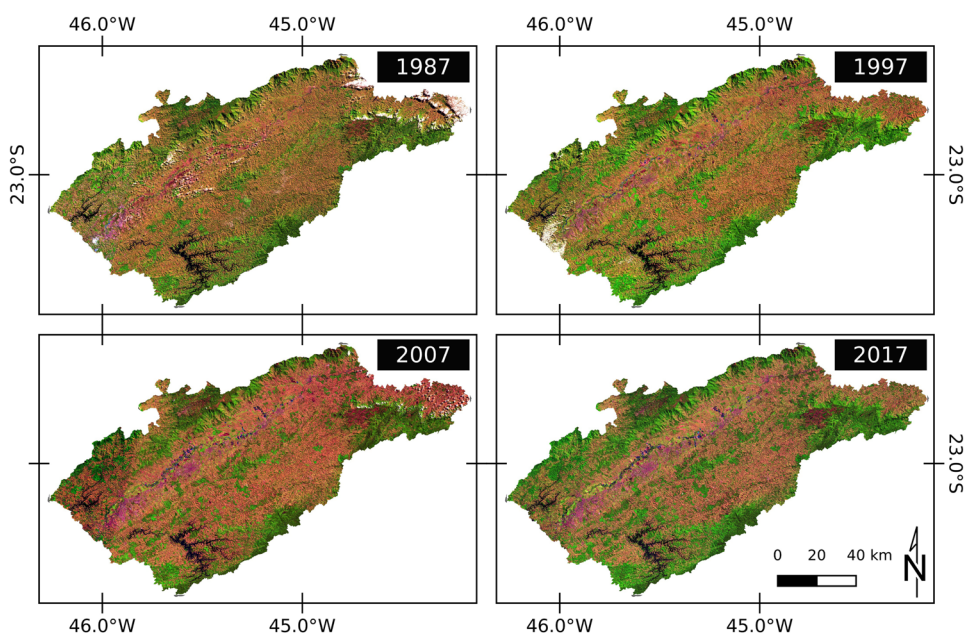
Fig. 3 Experiment design flowchart

particular, the following pair-wise years were considered: 1987–1997; 1997–2007; 2007–2017; and 1987–2017.

Different parameter settings were tested for all the change detection methods. For the CVA approach, the parameter refers to the thresholding option in either Otsu or Kittler-Illinghworth algorithms. The values of h (squared region length) and p (number of principal components) for the PCA-KM were the following: $(h, p) \in \{(3, 3), (3, 5), (5, 5)\}$. Concerning the ASF approach, the number of iterations ranged from 1 to 7. Notice that, for PCA-KM method, h has been limited to 5, as greater values for h may lead to feature spaces with very high dimensions, and consequently, computational prohibitive in face of the large image supports taken as input. Additionally, the values for p are limited by h, which have been empirically chosen after running successive experimental tests. Regarding the ASF method, it was observed from a preliminary battery

of tests that iterations above 7 provided over-smoothed and unrealistic change/non-change mappings.

Once the change maps were obtained, and the parameters properly defined, we computed the accuracy assessment of the results, by comparing the outputs produced by the change detection methods with the ground-truth samples (see Table 1). This was quantitatively assessed via the F1-Score measure, a statistical-based metric that balances the true/false positive/negative rates [39]. The higher the F1-Score, the better the results. Finally, the best results for each period was taken to conduct a more detailed investigation about the spatio-temporal dynamics of the study area.

The change detection methods were coded in IDL (Interactive Data Language), as well as the assessments presented in this study. Data and codes are freely available at https://github.com/rogerionegri/UCD.

Table 2 F1-Score computed for the change/non-change maps under different periods, methods and parameter settings. The highest scores are highlighted in italic

Method	Parameters	1987–1997	1997–2007	2007–2017	1987–2017
CVA	Otsu	0.004	0.004	0.006	0.017
	Kittler-Illing.	*0.887*	*0.970*	*0.983*	*0.860*
ASF	1 iteration	0.883	0.944	0.875	0.726
	2 iterations	0.752	0.826	0.832	0.428
	3 iterations	0.640	0.772	0.768	0.286
	4 iterations	0.457	0.536	0.650	0.161
	5 iterations	0.317	0.279	0.557	0.324
	6 iterations	0.304	0.058	0.299	0.322
	7 iterations	0.258	0.043	0.048	0.324
PCA-KM	(3,3)	0.120	0.004	0.006	0.017
	(3,5)	0.102	0.004	0.006	0.017
	(5,5)	0.102	0.004	0.006	0.017

Fig. 4 Change and non-change maps generated by the combination CVA + Kittler-Illinghworth algorithm for the periods of 1987–1997, 1997–2007, 2007–2017 and 1987–2017
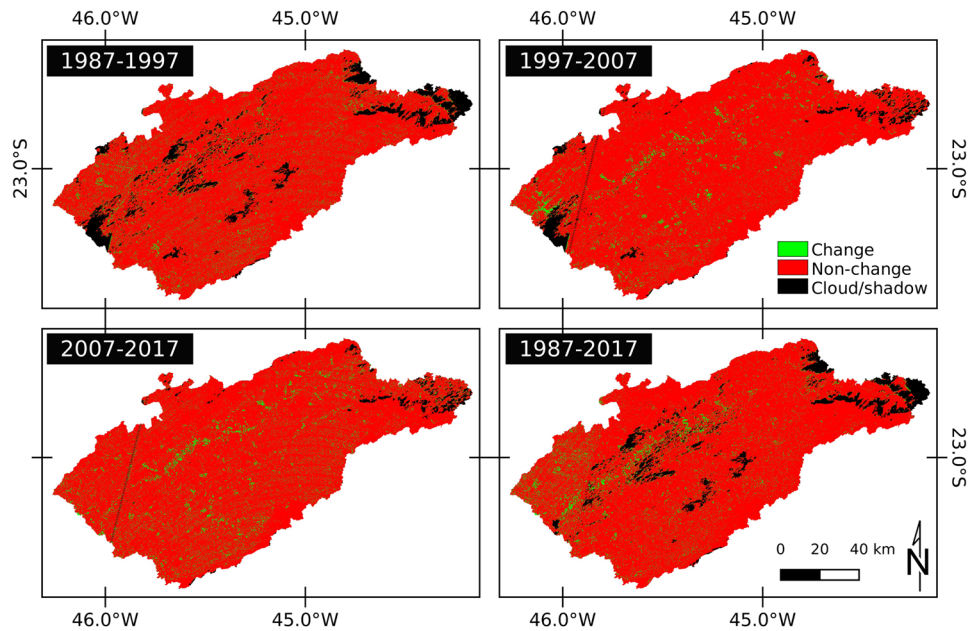
4 Results and Discussions

Following the experiment design (Subsection 3.2) and the multi-temporal data analysis (Subsection 3.1), a total of 48 change/non-change maps were generated (i.e., 4 periods × 12 methods/configurations). Table 2 shows the accuracy values, in terms of F1-Score, computed from these change detection maps.

From the tabulated scores in Table 2, one can verify that the PCA-KM approach produced the lowest values in comparison with the other change detection strategies. Although PCA-KM has been reported in the literature as a very robust approach, we have empirically observed that the low performance of the technique may be due to the high contrast elements (e.g., clouds occurrence), which impair the computation of suitable clusters of change and non-change events.

Regarding the ASF approach, there was an inverse relation between accuracy and number of iterations: the accuracy increases as the number of iteration decreases. Indeed,

this behavior is the result of successive applications of morphological operations. Also, notice that if one takes a single iteration, the ASF produces similar scores to the CVA method.

At last, one can see that the CVA approach (equipped with the Kittler-Illinghworth algorithm) achieves the highest accuracies in the study area. On the other hand, by applying the Otsu algorithm, the CVA technique delivered poor results. These are similar to the ones produced by PCA-KM for 1997–2007, 2007–2017 and 1987–2017 periods. Such a behavior may be explained by the occurrence of significant contrast differences, including pixel interferences after computing the best cutting-point by the Otsu algorithm.

Despite its simplistic architecture, the CVA turns out to be a very effective method for detecting changes in spatial-temporal images. Furthermore, the presence of clouds does not seem to influence the results achieved by "CVA + Kittler-Illinghworth" approach. Another interesting aspect to be observed is that from 1987 to 2017, the CVA

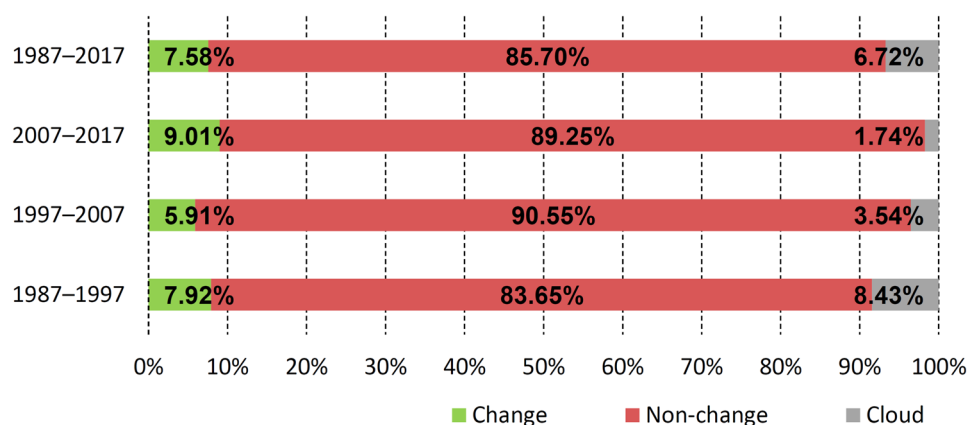**Fig. 5** Change and non-change percentage occurrences for each period

Table 3 Multi-temporal transitions summary and color legend key

1987-1997	ω_c	ω_c	ω_n	ω_c	ω_n	ω_c	ω_n	ω_n	Cloud
1997-2007	ω_c	ω_c	ω_c	ω_n	ω_c	ω_n	ω_n	ω_n	
2007-2017	ω_c	ω_n	ω_c	ω_c	ω_n	ω_n	ω_c	ω_n	
%	0.27	0.78	1.57	1.42	2.94	5.39	5.04	73.42	9.18
Color legend	■	■	■	■	■	■	■	■	■

delivered the lowest accuracy among all the examined periods. This performance reduction comes from the use of images acquired by different sensors (i.e., TM and OLI).

Once the CVA has been numerically attested as the most effective approach to cope with the study area, we perform visual inspections by taking the change/non-change maps as obtained by such method. Figure 4 presents the CVA results for all the evaluation periods. One can observe for each pair-wise comparison that the percentage of non-change is dominant. Also, notice that the changes are represented by small regions that are spread over all the study area, especially along the southeastern-northwest track. This portion contains the main highway that crosses the study area, which has led to a dense occupation, urban expansion and industrial activities. In fact, as pointed out by Andrade et al. [40], it was observed a great urban expansion between 1995 and 2015, when urbanized areas reached an increase of 133%. According to Silva et al. [8], demographic and market shifts have resulted in rural land abandonment over the last years and some lands transitioned to industrial production in the Paraíba do Sul River Valley, especially in areas near to cellulose and paper industries. Finally, Silva et al. [41] reinforce that urbanization, international market demands, industrialization and agricultural modernization are the main factors related to landscape changes in Atlantic Forest over the last decades.

Additionally, historical events reveled that this spatial behavior comes from the forest transition stage over the years, as it comprises the period from the permanent reduction of native vegetation to the gradual revitalization of the forest. Such an environment transformation is mainly related to the
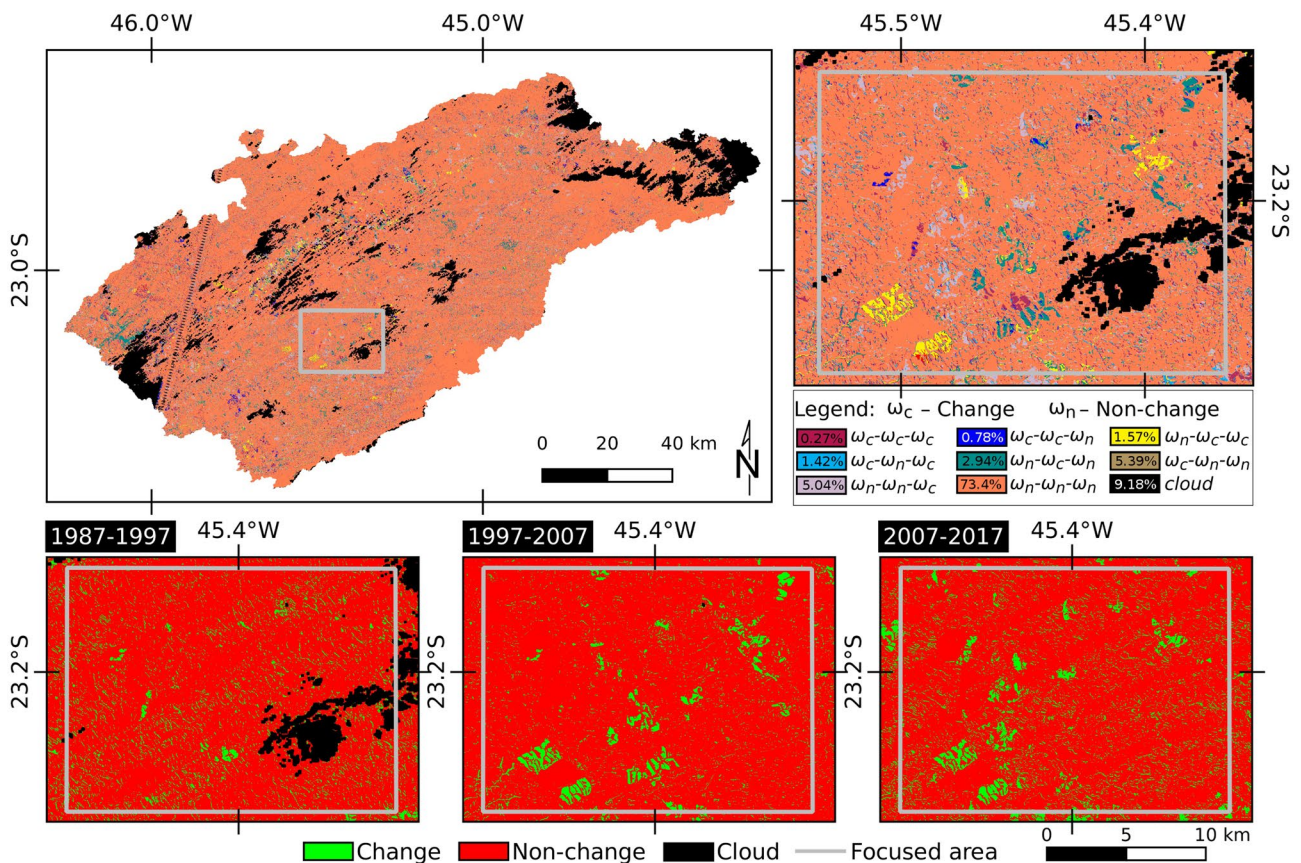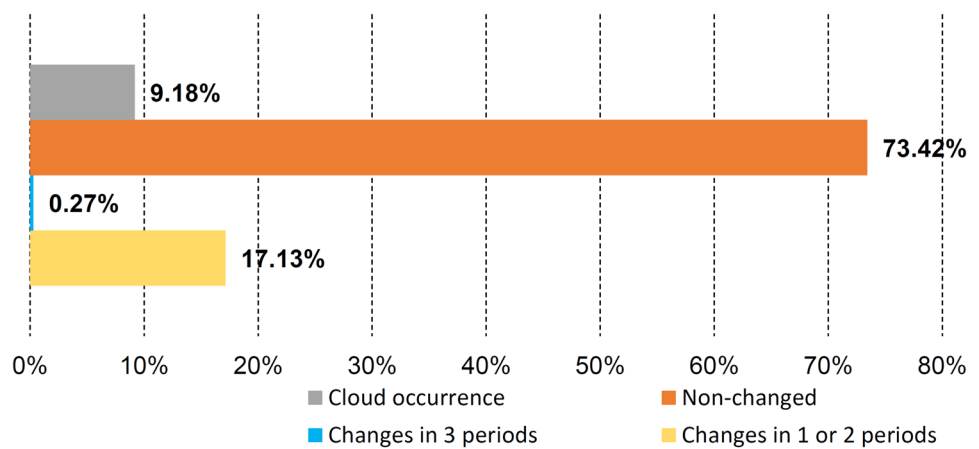

Fig. 6 Multi-temporal land cover transitions, in terms of a change/non-change sequence, over the period from 1987 to 2017

Fig. 7 General cases of multi-temporal transitions

abandonment of deep slope areas that were not compatible with mechanized agriculture, as well as local demographic and economic issues [8]. Another critical aspect is related to the increase in eucalyptus crop areas, as a consequence of the cellulose industries hosted in the region [7].

The scores in Fig. 5 brings a comparison – in terms of area percentage – between change and non-change regions, as well as the parcel compromised by cloud occurrence. In general, the change/non-change percentages are similar in all periods. If we disregard the cloud locations, it is revealed that on average a 92% of study area does not change from 1987 to 2017.

Although the findings about the change percentage in 1987-2017, such analysis does not take into account the land cover iterations occurred in particular years of this period. In order to address this issue, a step-by-step multi-temporal analysis can lead to a better understanding of the study area dynamics. In order to do so, we first compute the map of multi-temporal land cover transitions, which is depicted in Fig. 6, and next we quantify these transition occurrences, as listed in Table 3.

By grouping the eight transitions in Fig. 6 (and Table 3) into four general cases, which comprises cloud cover, non-changes, changes in one/two periods, and changes in three periods, one may verify that 73.42% of the clusters refers to non-change areas. Figure 7 shows the frequency distribution of the established classes.

Furthermore, if cloud-covered areas are unconsidered, the non-change percentage drops to 66.68%. This value represents a difference of 25.32% when the dynamics of the changes are examined in a pair-wise approach, thus revealing that the Paraíba do Sul River Valley has faced intermittent changes during the last decades.

5 Conclusions

Unsupervised learning for change detection is capable of providing significant visual insights of the spatial-temporal dynamics between multi-temporal images. Moreover, these

mappings can be handled and fused to obtain intuitive, multi-temporal representations of changes in the target region.

By taking such a remote sensing apparatus, we tracked the spatial-temporal changes in the Paraíba Valley along four decades, a southwestern Brazilian region which houses the Atlantic Forest biome. The changes were captured by applying different unsupervised change detection approaches, in an effort to find out the best strategy to identify disturbed areas in Atlantic Forest. We verified that the classic and well-established Change Vector Analysis method, when equipped with Kittler-Illinghworth thresholding approach, produced the best results in comparison with other analyzed methods.

The obtained results have also reveled a regular land-cover change rate about 8% under similar periods, i.e., 1987–1997, 1997–2007, 2007–2017 and 1987–2017. However, after the multi-temporal analysis with the integrated periods and disregarding cloud-covered areas, it was observed an increase of 33% w.r.t. changes over the three analyzed decades.

As future work, we plan to: (i) investigate the use of other thresholding strategies on the CVA algorithm, similar to the analysis conducted in [42], as we have found from our battery of tests that CVA provides accurate results when applied on the analyzed areas so that the thresholding value seems to play an important role in the the generated outputs; and (ii) decrease the temporal scale to five or less years, in an attempt to detect particular changes that may not have been captured when using multi-temporal dataset of ten-years steps, as properly discussed in the survey [43].

Author Contributions G. R. Sapucci: conceptualization, methodology, validation, and writing the original draft; R. G. Negri: conceptualization, methodology, software, validation, editing, and supervision; W. Casaca: validation and editing; K. G. Massi: validation, editing, and supervision.

Data Availability Statement Data and codes are freely available at https://github.com/rogerionegri/UCD.

Declarations

Conflict of Interest The authors declare that they have no conflict of interest.

References

1. Gomes, C., Reschilian, P. R., & Uehara. A. Y. (2018) Perspectivas do planejamento regional do Vale do Paraíba e litoral norte: marcos históricos e a institucionalização da região metropolitana no Plano de Ação da Macrometrópole Paulista. *urbe. Revista Brasileira de Gestão Urbana*, 10:154 – 171, 04. https://doi.org/10.1590/2175-3369.010.001.ao07

2. Myers, N., Mittermeier, R. A., Mittermeier, C. G., Fonseca, G. A. B., & Kent, J. (2000). Biodiversity hotspots for conservation priorities. *Nature,403*(6772), 853–858.

3. Cincotta, R., Wisnewski, J., & Engelman, R. (2000) Human populations in the biodiversity hotspots. *Nature*, 404:990–2, 05. https://doi.org/10.1038/35010105

4. Dean, W. (1997) *A Ferro e Fogo: A Historia da Devastação da Mata Atlantica Brasileira*. Companhia das Letras São Paulo.

5. Wu, C., Du, B., & Zhang, L. (2014). Slow Feature Analysis for Change Detection in Multispectral Imagery. *IEEE Transactions on Geoscience and Remote Sensing, 52*(5), 2858–2874. https://doi.org/10.1109/TGRS.2013.2266673

6. (2017) SMA. Atlas Dos Remanescentes Florestais da Mata Atlantica: 2015-2016. techreport, Fundao SOS Mata Atlantica and National Institute for Space Research, Sao Paulo, Brazil. https://www.sosma.org.br/wp-content/uploads/2019/05/Atlas-mata-atlantica_17-18.pdf

7. Itani, M. R., Barros, C. M., Figueiredo, F. E. L., Andrade, M. R. M., Mansor, M. T. C., Mangabeira, R. L., & Carvalho, V. S. (2011) Subsídios ao planejamento ambiental: Unidade de Gerenciamento de Recursos hídricos Paraíba do Sul–UGRHI 02 – Subsidies for Environmental Planning: Hydrographic Unit Water of Resources Management of Paraíba do Sul–UGRHI 02. techreport, Sao Paulo State Environment Secretariat, Sao Paulo, Brazil. p. 204 http://arquivos.ambiente.sp.gov.br/publicacoes/2016/12/Subsidios_ao_Planejamento_Ambiental_UGRHI-021.pdf

8. Silva, R. F. B., Batistella, M., & Moran, E. F. (2017). Socioeconomic changes and environmental policies as dimensions of regional land transitions in the atlantic forest, brazil. *Environmental Science & Policy,74*, 14–22.

9. Amitrano, D., Guida, R., & Iervolino, P. (2020) Semantic unsupervised change detection of natural land cover with multitemporal object-based analysis on sar images. *IEEE Transactions on Geoscience and Remote Sensing*, pages 1–21. https://doi.org/10.1109/TGRS.2020.3029841

10. Fazel, M. A., Homayouni, S., & Amini, J. (2013) Kernel-based unsupervised change detection of agricultural lands using multi-temporal polarimetric sar data. *ISPRS - International Archives of the Photogrammetry, Remote Sensing and Spatial Information Sciences*, XL-1/W3:169–173. DOI 10.5194/isprsarchives-XL-1-W3-169-2013. https://www.int-arch-photogramm-remote-sens-spatial-inf-sci.net/XL-1-W3/169/2013/

11. Durieux, A. M. S., Calef, M. T., Arko, S., Chartrand, R., Kontgis, C., Keisler, R., et al. (2019). Monitoring forest disturbance using change detection on synthetic aperture radar imagery. In M. E. Zelinski, T. M. Taha, J. Howe, A. A. S. Awwal, & K. M. Iftekharuddin (Eds.), *Applications of Machine Learning* (pp. 307–320)., volume 11139 SPIE: International Society for Optics and Photonics. https://doi.org/10.1117/12.2528945

12. Hame, T., Heiler, I., & Miguel-Ayanz, J. S. (1998). An unsupervised change detection and recognition system for forestry. *International Journal of Remote Sensing,19*(6), 1079–1099. https://doi.org/10.1080/014311698215612

13. Lei, T., Xue, D., Lv, Z., Li, S., Zhang, Y., & Asoke, K. N. (2018). Unsupervised change detection using fast fuzzy clustering for landslide mapping from very high-resolution images. *Remote Sensing,10*(9). https://doi.org/10.3390/rs10091381

14. Sublime, J., & Kalinicheva, E. (2019). Automatic post-disaster damage mapping using deep-learning techniques for change detection: Case study of the tohoku tsunami. *Remote Sensing,11*(9). https://doi.org/10.3390/rs11091123. https://www.mdpi.com/2072-4292/11/9/1123

15. Sathya, N., Kalaiselvi, S., Gomathi, V., and Srinivasagan, K. G. (2014) Unsupervised monitoring of urban land use and land cover change detection in multitemporal images. In *2014 International Conference on Electronics and Communication Systems (ICECS)*, pages 1–5. DOI 10.1109/ECS.2014.6892722

16. USGS. United States Geological Survey. EarthExplorer platform and EROS data center. U.S. Dept. of the Interior, U.S. Geological Survey, 2019.

17. Seto, K. C., Woodcock, C., Song, C., Huang, X., Lu, J., & Kaufmann, R. (2002). Monitoring land-use change in the pearl river delta using landsat tm. *International Journal of Remote Sensing,23*(10), 1985–2004.

18. Lu, D., Mausel, P., Brondizio, E., & Moran, E. (2004). Change detection techniques. *International journal of remote sensing,25*(12), 2365–2401.

19. Mura, M. D., Benediktsson, J. A., Bovolo, F., & Bruzzone, L. (2008). An unsupervised technique based on morphological filters for change detection in very high resolution images. *IEEE Geoscience and Remote Sensing Letters,5*(3), 433–437.

20. Du, B., Ru, L., Wu, C., & Zhang, L. (2019). Unsupervised deep slow feature analysis for change detection in multi-temporal remote sensing images. *IEEE Transactions on Geoscience and Remote Sensing,57*(12), 9976–9992.

21. Negri, R. G., Frery, A. C., Casaca, W., Azevedo, S., Dias, M. A., Silva, E. A., & Alcantara, E. H. (2020) Spectral-spatial-aware unsupervised change detection with stochastic distances and support vector machines. *IEEE Transactions on Geoscience and Remote Sensing*, pages 1–14.

22. Webb, A. R., & Copsey, K. D. (2011) *Statistical pattern recognition*. John Wiley & Sons, Chichester, 3rd ed. edition.

23. Johnson, R. D., & Kasischke, E. S. (1998). Change vector analysis: a technique for the multispectral monitoring of land cover and condition. *International Journal of Remote Sensing,19*(3), 411–426.

24. Otsu, N. (1979) A threshold selection method from gray-level histograms. *IEEE Trans. on Systems, Man, and Cybernetics*, 9(1):62–66. https://doi.org/10.1109/TSMC.1979.4310076

25. Kittler, J., & Illingworth, J. (1986). Minimum error thresholding. *Pattern Recognition,19*(1), 41–47. https://doi.org/10.1016/0031-3203(86)90030-0

26. Jolliffe, I. (2011). *Principal component analysis*. Springer.

27. Deng, J. S., Wang, K., Deng, Y. H., & Qi, G. J. (2008). Pca-based land-use change detection and analysis using multitemporal and multisensor satellite data. *International Journal of Remote Sensing,29*(16), 4823–4838. https://doi.org/10.1080/01431160801950162

28. Martinez-Izquierdo, M. E., Molina-Sanchez, I., and M.-B. M. C. (2019) Efficient dimensionality reduction using principal component analysis for image change detection. *IEEE Latin America Transactions*, 17(04):540–547.

29. Song, M., Zhong, Y., Ma, A., & Zhang, L. (2017) Unsupervised change detection for remote sensing images based on principal component analysis and differential evolution. In Y. Shi, K. C. Tan, M. Zhang, K. Tang, X. Li, Q. Zhang, Y. Tan, M. Middendorf, and Y. Jin, editors, *Simulated Evolution and Learning*, pages 786–796. Springer International Publishing.

30. Celik, T. (2009). Unsupervised change detection in satellite images using principal component analysis and *k*-means clustering. *IEEE Geoscience and Remote Sensing Letters,6*(4), 772–776.

31. Vecchi, D., Galeazzo, D. A., Harb, M., & Dell'Acqua, F. (2015) Unsupervised change detection for urban expansion monitoring: An object-based approach. In *2015 IEEE International Geoscience and Remote Sensing Symposium (IGARSS)*, pages 350–352. https://doi.org/10.1109/IGARSS.2015.7325772

32. Azevedo, S. A., S. E. A., Colnago, M., Negri, R. G., & Casaca, W. (2019) Shadow detection using object area-based and morphological filtering for very high-resolution satellite imagery of urban areas. *Journal of Applied Remote Sensing*, 13(3):1 – 16. https://doi.org/10.1117/1.JRS.13.036506

33. Gonzalez, R. C., & Woods, R. E. (2017) *Digital image processing*. Pearson, 4th edition, 2017.

34. (2019) IBGE. Demographic data 2010. The Brazilian Institute of Geography and Statistics (Instituto Brasileiro de Geografia e Estatastca). URL www.ibge.gov.br

35. (2019) USGS: United States Geological Survey. EarthExplorer platform and EROS data center.U.S. Dept. of the Interior, U.S. Geological Survey. earthexplorer.usgs.gov

36. (2019) USGS. Product guide: Landsat 4-7 ecosystem disturbance adaptive processing system (LEDAPS). techreport, United States Geologycal Service. Accessed on 1 August 2019. https://www.usgs.gov/media/files/landsat-4-7-surface-reflectance-code-ledaps-product-guide

37. (2017) USGS. Product guide: Landsat 8 surface reflectance code (LASRC) product. techreport, United States Geologycal Service. Accessed on 1 August 2019. https://www.usgs.gov/media/files/land-surface-reflectance-code-lasrc-product-guide

38. Souza, C. M., Shimbo, J. Z., Rosa, M. R., Parente, L. L., Alencar, A. A., Rudorff, B. F. T., et al. (2020). Reconstructing three decades of land use and land cover changes in brazilian biomes with landsat archive and earth engine. *Remote Sensing,12*(17), DOI 10.3390/rs12172735. https://www.mdpi.com/2072-4292/12/17/2735

39. Rijsbergen, C. J. V. (1979). *Information Retrieval* (2nd ed.). Newton, MA, USA: Butterworth-Heinemann.

40. Andrade, D. J, Souza, A. A. M., & Gomes, C. (2019). Temporal analysis of urban expansion in the municipalities of the paraíba paulista valley. *Mercator (Fortaleza)*, 18.

41. Silva, R. F. B., Batistella, M., Moran, E. F., & Lu, D. (2017). Land changes fostering atlantic forest transition in brazil: Evidence from the paraba valley. *The Professional Geographer,69*(1), 80–93. https://doi.org/10.1080/00330124.2016.1178151

42. R. Singh, S. & Talwar (2015). Performance analysis of different threshold determination techniques for change vector analysis. *Journal of the Geological Society of India*, 86(86):52–58. https://doi.org/10.1007/s12594-015-0280-x

43. Aplin, P. (2006). On scales and dynamics in observing the environment. *International Journal of Remote Sensing,27*(11), 2123–2140. https://doi.org/10.1080/01431160500396477